Ubiquitination is a novel post-translational modification of VMP1 in autophagy of human tumor cells

Felipe J. Renna[1], Juliana H. Enriqué Steinberg[2], Maria Manifava[3], Claudio D. Gonzalez[1], Mariana S. Tadic[1], Tamara Orquera[1], Carolina V. Vecino[1], Alejandro Ropolo[1], Mario Rossi[2], Nicholas T. Ktistakis[3], Maria I. Vaccaro[1]*

[1] Universidad de Buenos Aires, CONICET, Instituto de Bioquimica y Medicina Molecular Prof Alberto Boveris (IBIMOL), Buenos Aires, Argentina; mvaccaro@ffyb.uba.ar
[2] Universidad Austral, CONICET, Instituto de Investigaciones en Medicina Traslacional (IIMT), Pilar, Argentina; mrossi-conicet@austral.edu.ar
[3] Signalling Programme, Babraham Institute, Cambridge, UK; nicholas.ktistakis@babraham.ac.uk

* Correspondence: mvaccaro@ffyb.uba.ar

Abstract: Autophagy is a tightly regulated catabolic process involved in the degradation and recycling of proteins and organelles. Ubiquitination plays an important role in the regulation of autophagy. Vacuole Membrane Protein 1 (VMP1) is an essential autophagy protein whose expression in pancreatic cancer stem cells, carrying activated Kirsten rat sarcoma viral oncogene homolog (KRAS), triggers autophagy and enables therapy resistance. Using biochemical and cellular approaches we identified ubiquitination as a post-translational modification of VMP1 from the initial steps in autophagosome biogenesis, remaining ubiquitinated as part of the autophagosome membrane throughout autophagic flux until autolysosome formation. However, VMP1 is not degraded by autophagy nor by the ubiquitin-proteasomal system. Mass spectrometry and immunoprecipitation showed that Cell division cycle protein cdt2 (Cdt2), the substrate recognition subunit of the E3 ligase complex associated with cancer Cullin–RING ubiquitin ligase complex 4 (CRL4), is a novel interactor of VMP1 and is involved in VMP1 ubiquitination. VMP1 ubiquitination decreases under the CRL inhibitor MLN4924 and increases with the Cdt2 overexpression. Our results indicate that ubiquitination is a novel post-translational modification of VMP1 during autophagy in human tumor cells. VMP1 ubiquitination may be of clinical relevance in tumor cell therapy resistance.

Keywords: Autophagy; Cancer; Ubiquitination; VMP1

1. Introduction

Macroautophagy (commonly mentioned as autophagy) is a physiological catabolic process that allows protein degradation and organelles turnover through lysosomal degradation. During this process, the autophagosome, a specific double membrane vesicle, is formed. It sequesters the cargo molecules driving them to the lysosome for degradation by hydrolytic enzymes [1,2]. Since autophagy is essential for cellular homeostasis maintenance, diverse stimuli are integrated in a complex network of signals, leading to autophagy induction. In this way, the cell is able to respond to stressors such as amino acids starvation, low energetic levels, reticulum stress, hypoxia and oxidative stress triggering autophagy to repair damaged structures or to obtain energy sources [2]. Mechanistically, the autophagy pathway is orchestrated by a large set of evolutive conserved proteins, known as autophagy-related proteins (ATG), which allows the autophagosome formation and the complete development of the process [3]. Given the high complexity in the molecular mechanisms that govern autophagy and the essentiality of this process, it presents a tight regulation. This regulation is not only related to the vast induction pathway network, but also to the activity of each singular ATG protein. Post-translational modifications play an important role modulating protein interactions, destination, and catalytic activity in enzymatic proteins [4]. Ubiquitination is one of the most complex and versatile posttranslational modifications [5].

During autophagy induction, several stress signals are integrated by two protein kinases: Mammalian target of rapamycin (mTOR) and AMP activated protein kinase (AMPK). These signals lead to AMPK activation and/or mTOR inhibition [2]. The next step in the autophagic pathway is the activation of the ULK1 complex. This complex is integrated by the proteins ATG13, FAK family interacting protein of 200kDa (FIP200), ATG101 and the protein kinase ULK1, that works as a serine/threonine protein kinase leading to the phosphorylation and activation of downstream substrates [6]. Downstream to the ULK1 Complex, the phosphatidylinositol 3-kinase type 3 complex 1 (PI3KC3-C1) is composed of the proteins Beclin 1 (BECN1), ATG14L, Serine/Threonine protein kinase VPS15 (Vps15) and Phosphatidylinositol 3-kinase VPS34 (Vps34), the catalytic subunit, which produces Phosphatidylinositol 3-phosphate (PI3P) in the site where the autophagosome begins to sprout [7]. This event results in the recruitment of PI3P-binding proteins, such as Double FYVE-containing protein 1 (DFCP1) and WD40-repeat phosphoinositide-interacting protein 2 (WIPI2) and is followed by the recruitment of the ATG12-ATG5-ATG16L complex allowing the lipidation of microtubule-associated protein 1 light chain 3 (LC3) with phosphatidylethanolamine (PE) [1,2]. After LC3 lipidation, cargo molecules are enveloped, the membrane is elongated and the autophagosome finally sprouts. In the last part of this process, the autophagosome is fused with the lysosome in a process dependent on Syntaxin-17 (STX17) and Ras-related protein Rab-7a (RAB7), forming the autolysosome and leading to cargo degradation [8,9].

Ubiquitination (or ubiquitylation) consists in a covalent modification with one or more molecules of ubiquitin. Ubiquitin is a 76 amino acids length protein that is highly conserved in eukaryotic organisms. Ubiquitination takes place through the sequential action of three enzymes: the ubiquitin-activating enzyme (E1), the ubiquitin-conjugating enzyme (E2) and the ubiquitin protein ligase (E3) [10,11]. Ubiquitination presents a huge versatility given ubiquitin can be added as a simple molecule (monoubiquitination) or as polymeric ubiquitin chains, presenting diverse variants.

Ubiquitination plays an essential role in autophagy regulation since most of the autophagy-related proteins are regulated by ubiquitination, leading them to proteasomal degradation or activating their function [5]. Ubiquitination mechanisms are implicated in the regulation of every stage of the autophagic process, allowing a more precise and faster adaptation to the microenvironmental conditions. Moreover, ubiquitination is also implicated in the cargo labelling for selective types of autophagy [5].

Vacuole Membrane Protein 1 (VMP1) is a 406 amino acids transmembrane protein [12] whose expression induces autophagy in mammalian cells [13,14]. VMP1 interacts with BECN1 allowing the recruitment of the PI3KC3 Complex 1 to the site of autophagosome formation [13,14] in the Endoplasmic Reticulum (ER)-Plasma Membrane (PM) contact sites [15]. VMP1 is essential for autophagy [13] given in absence of VMP1 expression, autophagosomes remain attached to the endoplasmic reticulum not being able to continue with the autophagic flux [16]. Moreover, VMP1 has been found to be part of the membrane of isolated autophagosomes in the context of the cellular response to acute pancreatitis [17,18]. Recently, by *in vitro* reconstitution assays, VMP1 has been proposed to have lipids scramblase activity [19], which adds complexity to its function and increases even more its relevance as a vesicle trafficking protein.

The role of VMP1 is remarkably important in the cellular response to the disease. VMP1 expression is not detectable in healthy human pancreas, but it is markedly triggered in response to pancreatitis [12,13], diabetes [20] and pancreatic cancer [21,22]. Under acute pancreatitis-induced stress VMP1 expression triggers zymophagy, the selective autophagy of activated zymogen granules [17] and mitophagy, the selective autophagy of damaged mitochondria [23], playing a protective role and avoiding the progression to a severe disease. In pancreatic cancer cells, VMP1 expression is induced by mutated KRAS [24]. We recently showed that VMP1 expression is activated by gemcitabine treatment through E2F1 transcription factor, triggering autophagy and mediating chemotherapy resistance [21,22]. Also, VMP1 is involved in the resistance to photodynamic therapy in colon cancer cells, in which its expression is triggered by the transcription factor Hypoxia-inducible factor 1 alpha (HIF-1α) [25]. Therefore, VMP1 plays a relevant role in tumor pathophysiology. Given the important role of VMP1 in the autophagy pathway, in pancreatic pathophysiology and in tumor resistance mechanisms, VMP1 should be tightly regulated not only at the transcriptional level, but also at the post-translational one.

Previously, VMP1 has been found to co-distribute with ubiquitin in immunofluorescence experiments [26]. In this study, we used tumoral cells as an experimental model to study the ubiquitination of VMP1. We identified the ubiquitination as a post-translational modification for VMP1, which does not label it for degradation in the proteasome nor by autophagy. VMP1 is ubiquitinated early in autophagosome biogenesis and remains ubiquitinated as part of the autophagosome membrane throughout the autophagic flux until autolysosome formation. Moreover, Cdt2 (Cell division cycle protein cdt2), the substrate recognition subunit of the Cullin–RING ubiquitin ligase complex 4 (CRL4), interacts with VMP1. We found that the CRL4/Cdt2 E3 ligase is involved in VMP1 ubiquitination as a novel post-translational modification, which might be relevant during the autophagic pathway in human tumor cells.

2. Results

2.1. VMP1 is post-translationally modified by ubiquitination

We performed immunofluorescence of ubiquitin in HeLa cells transfected with VMP1-GFP. The number of ubiquitin dots per cell in VMP1-GFP transfected cells was significantly higher in comparison to non-transfected or Enhanced Green Fluorescent Protein (GFP) transfected cells, indicating that the expression of VMP1 induces ubiquitin recruitment (Figure 1A). These data were confirmed in other tumor cell lines, PANC-1 (Figure S1) and MCF-7 (Figure S2). In these images we observed that ubiquitin dots distribution coincides with VMP1 distribution. Then, we performed immunofluorescence of ubiquitin in VMP1-GFP transfected HEK293T cells and determined the colocalization between VMP1 and Ubiquitin. Figures 1B-D show that VMP1-GFP expression significantly colocalized with ubiquitin (Ub) under starvation as well as under nutrient replete conditions. To evaluate if VMP1 is ubiquitinated we performed immunoprecipitation with anti-FLAG in lysates from VMP1-GFP and FLAG-Ub co-transfected cells. Immunoblotting of eluates with anti-FLAG showed the presence of a big set of ubiquitinated proteins. Immunoblotting with anti-VMP1 showed several bands corresponding to VMP1-GFP and ubiquitinated VMP1-GFP, suggesting that VMP1 is poli-ubiquitinated. Also, a band around 85 kDa, that could be compatible with monoubiquitination, appears in Figure 1E. Then, we performed immunoprecipitation using anti-V5 in lysates from VMP1-V5 and FLAG-Ub co-transfected cells. Immunoblotting with anti-V5 shows bands corresponding to VMP1-V5 and ubiquitinated VMP1-V5. Immunoblotting with anti-FLAG show bands corresponding to VMP1-V5 ubiquitination (Figure 1F). These results demonstrate that VMP1 is modified by ubiquitination.

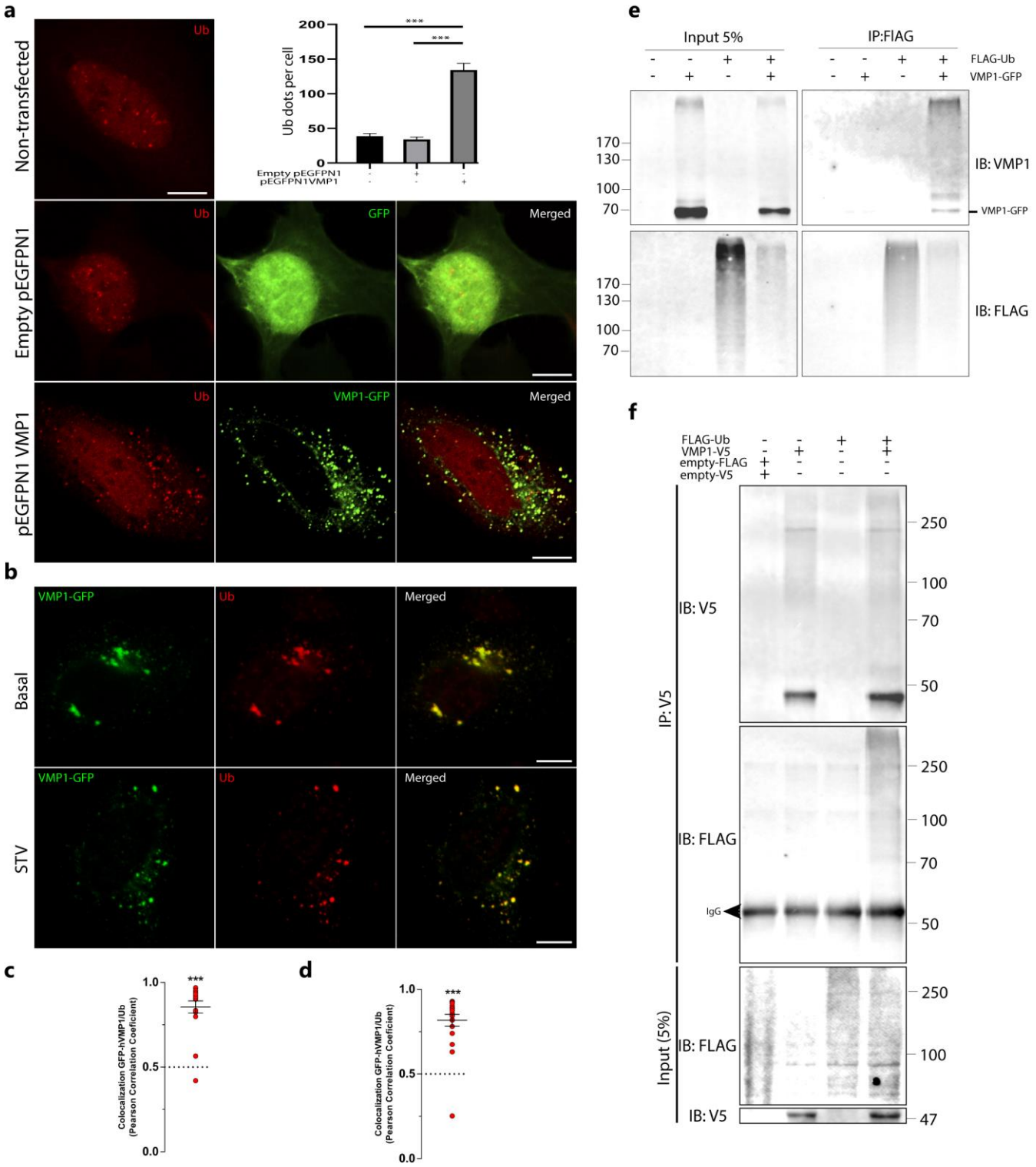

Figure 1. VMP1 is post-translationally modified by ubiquitination. (**a**) HeLa cells expressing Empty pEGFPN1 or pEGFPN1 VMP1, or non-transfected HeLa cells, were immunolabeled with anti-ubiquitin. Scale bars: 10 µm. The number of ubiquitin (Ub) dots per cell was quantified in at least 12 individual cells per condition in three independent experiments. The means per condition and the SEM are represented in the graphic. ***: p<0.001 by Kruskall-Wallis test. (**b**) HEK293T cells were transfected with VMP1-GFP and immunolabeled with anti-ubiquitin in basal and starvation (1h) conditions. Scale bars: 10 µm. Basal: Cells transfected with VMP1-GFP. GFP: Green Fluorescent Protein. STV: Cells transfected with VMP1-GFP and starved. (**c**) (**d**) Colocalization between VMP1 and ubiquitin was quantified in individual cells under basal (n=17) (**c**) and starvation (n=20) (**d**) conditions in three independent experiments. In the graphics red plots show Pearson's Correlation Coefficient (PCC). ***p < 0.001 by two-tailed Student's t test vs the theoretical mean 0.5. (**e**) Lysates from HEK293T cells transfected with FLAG-Ub, VMP1-GFP and the combination of both were immunoprecipitated with anti-FLAG magnetic beads and immunoblotted with anti-VMP1. Several bands over VMP1-GFP molecular weight (73kDa) appear in the eluate of cotransfected cells indicating VMP1 ubiquitination. The image is representative of three independent experiments. (**f**) Lysates from HEK293T cells transfected with VMP1-V5, FLAG-Ub and the combination of both were

immunoprecipitated with anti-V5 magnetic beads and immunoblotted with anti-FLAG. Several bands over VMP1-V5 molecular weight (47.5 kDa) appear in the eluate of cotransfected cells indicating VMP1 ubiquitination.

To investigate if VMP1 is also modified by monoubiquitination, we concomitantly transfected cells with VMP1-GFP and Myc-Ub (wild type) or Myc-Ub (K0). Lysine free ubiquitin (K0 Ub) consists of a ubiquitin molecule whose lysine residues are replaced by arginine residues making the formation of chains impossible (Figure 2A). The cell lysates were immunoprecipitated with Anti-Myc linked Protein G – Sepharose and the eluates were immunoblotted with anti-GFP. We found that VMP1 is only ubiquitinated in presence of Myc-Ub (wild type) but not of Myc-Ub (K0) (Figure 2B). These results indicate that VMP1 is not monoubiquitinated and confirm that VMP1 is polyubiquitinated.

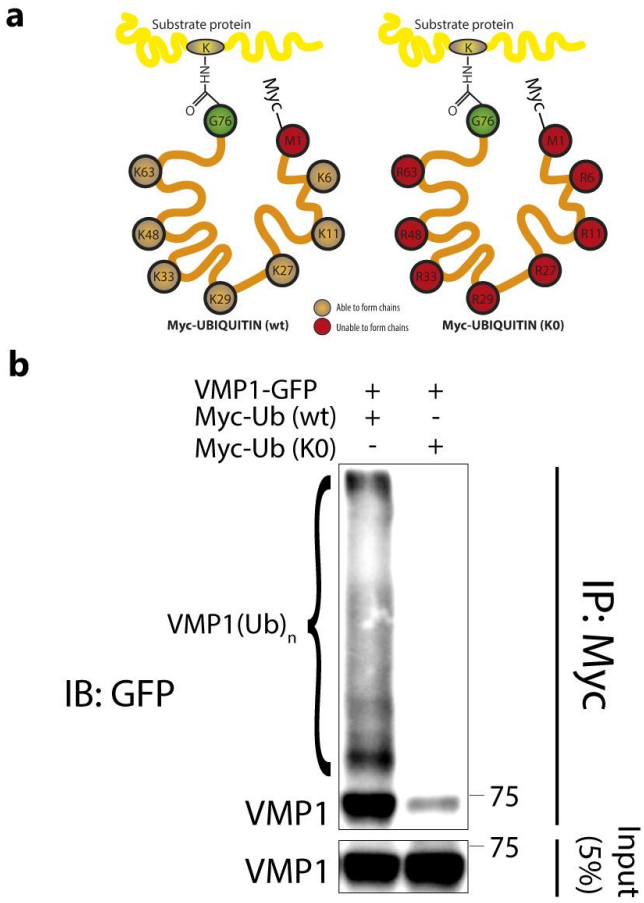

Figure 2. VMP1 is not monoubiquitinated with Myc-Ub (K0). (**a**) Schematic representation of Myc-Ub (K0) and Myc-Ub (wt) showing that Myc-Ub (K0) has the seven lysine residues replaced by arginine residues. In this way, Myc-Ub (K0) is only able to form monoubiquitination. (**b**) Lysates from HEK293T cells transfected with VMP1-GFP and Myc-Ub (wt) or Myc-Ub (K0) were immunoprecipitated with Anti-Myc linked to Protein G – Sepharose. The immunoblot with Anti-GFP shows there are no ubiquitination bands in the eluates from Myc-Ub (K0) expressing cells, indicating that VMP1 is not monoubiquitinated. In contrast, eluates from Myc-Ub (wt) expressing cells show several bands corresponding to polyubiquitination of VMP1. The image is representative of three independent experiments. K0 Ub: Lysine-free ubiquitin. Wt: Wild type.

2.2. Ubiquitinated VMP1 is not degraded by autophagy or ubiquitin-proteasome system

Given the ubiquitination of VMP1 might regulate its degradation, we aimed to analyze the degradation pathways for VMP1. In the first place, we tested if VMP1 is degraded by the proteasome. For this purpose, HEK293T cells were transfected with VMP1-GFP and treated with the proteasome inhibitor MG132 for 6 h. We observed that VMP1-GFP was not accumulated under proteasome inhibition (Figures 3A-B). As a control of the proteasome blocking, we quantified the levels of total ubiquitinated proteins showing their significant increase under MG132 treatment (Figure 3A, C). To confirm the obtained result, we performed a cycloheximide (CHX) chase assay in VMP1-GFP expressing cells treated with or without MG132. Results showed that VMP1-GFP levels decrease in a similar time course in presence or absence of MG132 (Figures 3D-G). As a set, these results indicate that ubiquitinated VMP1 is not degraded by the ubiquitin-proteasome system.

In the next step, we analyzed if VMP1 is degraded by autophagy. HEK293T cells were transfected with VMP1-GFP and treated with chloroquine (CQ) during 24 h. VMP1-GFP was not accumulated in chloroquine treated cells compared to non-treated cells (Figures 3H-I). Indeed, a little but significant decrease was found in VMP1-GFP. As a control of lysosome blocking, we show that LC3-II levels significantly increase under chloroquine treatment (Figure 3H, J). The absence of VMP1 accumulation in CQ

treated cells suggests that the ubiquitination of VMP1 does not drive it to degradation by autophagy. Then, we performed a cycloheximide chase assay in CQ treated cells. We observed that the time course decrease in VMP1 levels under CHX treatment (Figures 3K-L) is similar to the results obtained in cells without CQ treatment (Figures 3D-E). These results indicate that ubiquitinated VMP1 is not degraded by autophagy.

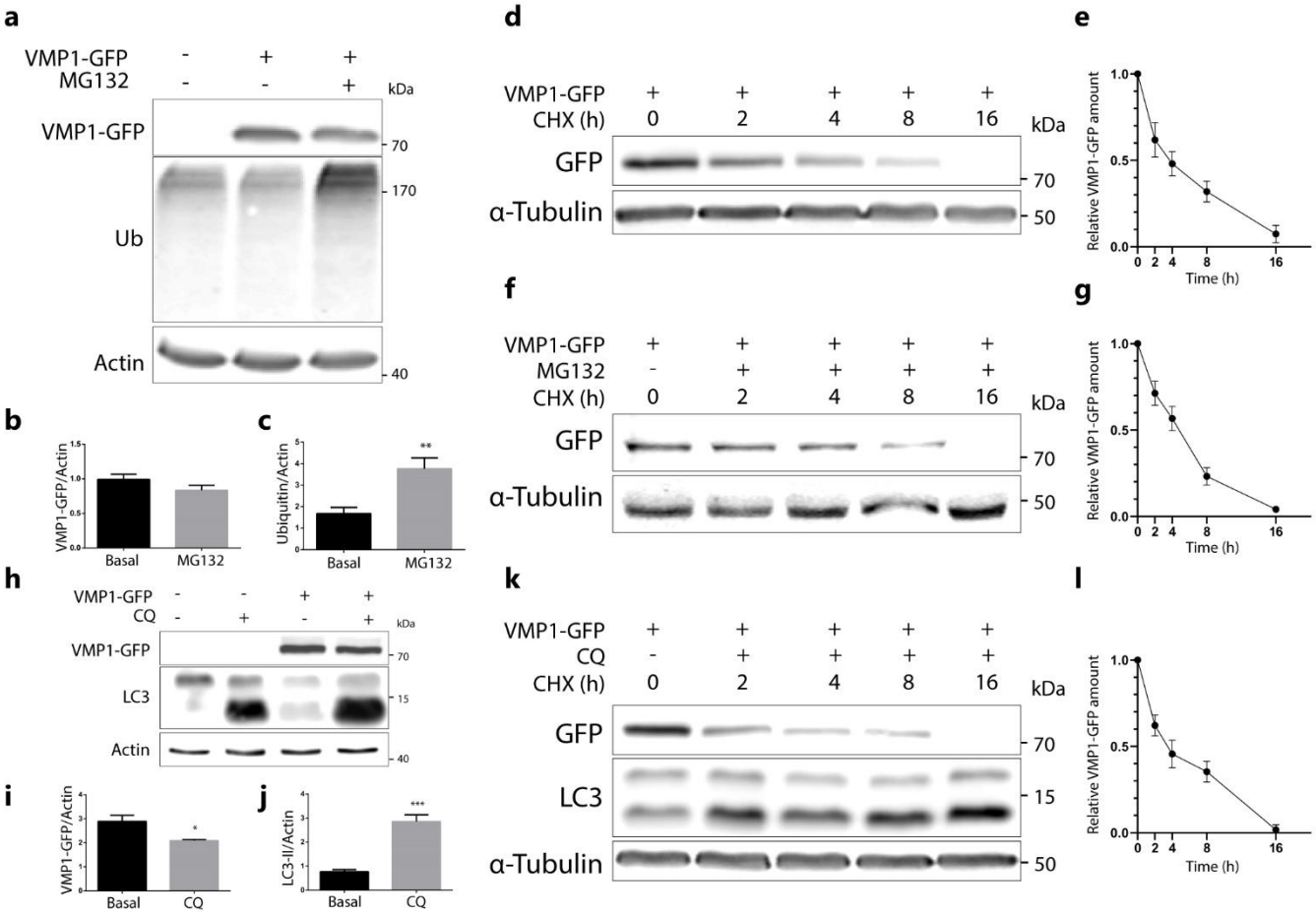

Figure 3. VMP1 is not degraded by the ubiquitin-proteasomal system nor by autophagy (**a**) Western blotting for VMP1, Ubiquitin and Actin where actin served as a loading control. HEK293T cells were transfected with VMP1-GFP and treated with or without the proteasome inhibitor MG132 (10uM) during 6h. Images are representative of three independent experiments (**b**) Quantification of relative densitometry shows VMP1-GFP (VMP1-GFP/Actin) does not change significantly after treatment with MG132. (**c**) Relative densitometry (Ubiquitin/Actin) shows that ubiquitin levels increase significantly after MG132 treatment, indicating the proteasome was effectively blocked. **$p < 0.01$ vs basal by Mann-Whitney nonparametric test. n=3. (**d**) Western blotting for GFP and α-Tubulin where α-Tubulin served as a loading control. HEK293T cells were transfected with VMP1-GFP and treated with cycloheximide (CHX) 100 ug/ml during 0, 2, 4, 8 or 16 h. Images are representative of three independent experiments. (**e**) The graphic shows the means and SEMs of relative densitometry (VMP1-GFP/ α-Tubulin) in relation with the relative densitometry for 0h. N=3 for each time. (**f**) Western blotting for GFP and α-Tubulin. HEK293T cells were transfected with VMP1-GFP and treated with CHX (100 ug/ml) and MG132 (10 μM) during 0, 2, 4, 8 or 16 h. Images are representative of three independent experiments. (**g**) The graphic shows the means and SEMs of relative densitometry (VMP1-GFP/ α-Tubulin) in relation with the relative densitometry for 0h. N=3 for each time. (**h**) Western blotting for VMP1, microtubule-associated protein 1 light chain 3 (LC3) and Actin where actin served as a loading control. HEK 293T cells were transfected with VMP1-GFP and treated with or without the lysosome inhibitor chloroquine (CQ) 50uM during 24h. Images are representative of three independent experiments. (**i**) Quantification of relative densitometry shows VMP1-GFP (VMP1-GFP/Actin) does not accumulate after treatment with CQ. In fact, VMP1-GFP significantly decreases in CQ treated cells. *$p < 0.1$ vs basal by Mann-Whitney nonparametric test. n=3 (**j**) Relative densitometry (LC3-II/Actin) shows that LC3-II levels significantly increase after CQ treatment, indicating that the lysosomal pathway was effectively blocked. ***$p < 0.001$ vs basal by Mann-Whitney nonparametric test. n=3. (**k**) Western blotting for GFP, LC3 and α-Tubulin. HEK293T cells were transfected with VMP1-GFP and treated with CHX (100 ug/ml) and CQ (100 μM) during 0, 2, 4 or 8 h, or CHX 100 (ug/ml) and CQ (50 μM) during 16 h. Images are representative of three independent experiments. (L) The graphic shows the means and SEMs of relative densitometry (VMP1-GFP/ α-Tubulin) in relation with the relative densitometry for 0h. N=3 for each time.

2.3. Ubiquitinated VMP1 is involved in the autophagic process

So far, we know that VMP1 is modified by ubiquitination and that ubiquitination does not initially lead to VMP1 degradation by proteosome or by autophagy. A large set of data showed that ubiquitination is crucial to regulate the autophagy related protein functions [5]. We therefore hypothesized that VMP1 ubiquitination could be related to its involvement in autophagy. We performed immunofluorescence of LC3 and Ubiquitin in VMP1-GFP transfected cells and we found that LC3 dots were mostly associated with ubiquitinated VMP1. Interestingly, in a perinuclear zone where VMP1 is not ubiquitinated, it did not recruit LC3 (Figure 4A-

B). Figure 4C shows the quantification of the LC3 dots associated with VMP1. While 76 % of LC3 dots were associated with ubiquitinated VMP1 (VMP1-Ub-LC3), only 2 percent of them were associated with no-ubiquitinated VMP1(VMP1-LC3). It is noteworthy that almost all VMP1 dots that colocalize with LC3, are associated with ubiquitin. We then used GFP-DFCP1, as a marker of omegasome in VMP1-DsRed transfected cells that were immunolabeled with anti-Ub. We found that while 35% of ubiquitinated VMP1 is associated with Double FYVE-containing protein 1 (DFCP1), DFCP1 is associated only with ubiquitinated VMP1 (VMP1-Ub-DFCP1) (Figure 4D-E). These findings suggest that VMP1 is ubiquitinated from the initial steps of autophagosome biogenesis.

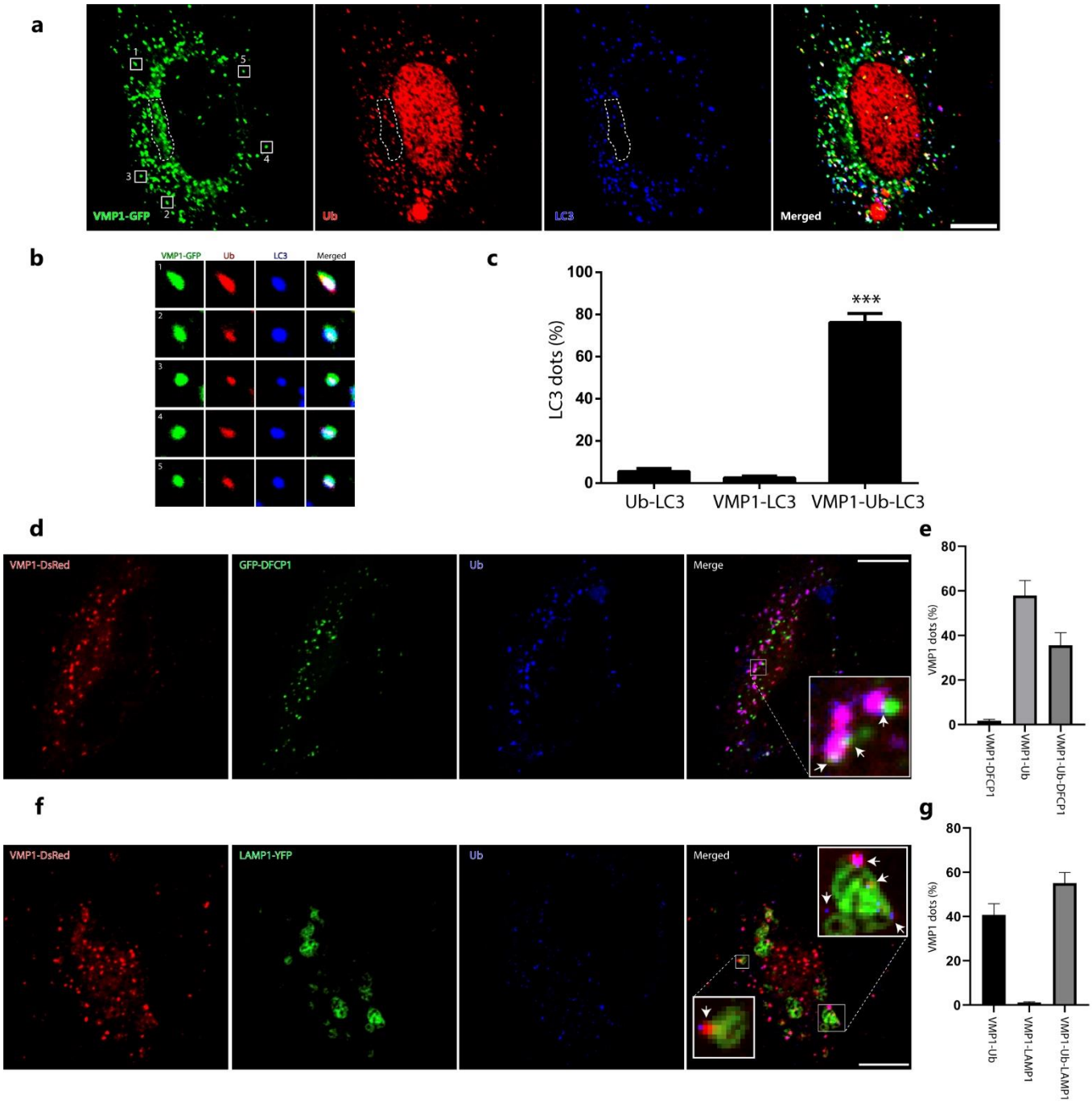

Figure 4. VMP1 associated with ubiquitin is involved in the autophagic process. (**a**) HeLa cells were transfected with VMP1-GFP and immunolabeled with anti-ubiquitin and anti-LC3. Scale bar: 10 µm. Images are representatives of three independent experiments. The area bounded by the dotted line shows a perinuclear zone where VMP1 that was not associated with Ub, did not recruit LC3. (**b**) Square magnifications show examples of VMP1 dots that are associated with Ub and LC3. (**c**) Quantification of LC3 dots per cell associated with ubiquitin, VMP1 or Ubiquitin and VMP1. ***$p < 0.001$ by two ways ANOVA vs. Ub and VMP1 groups. n=10 cells in 3 independent experiments. (**d**) HeLa cells were transfected with VMP1-DsRed, GFP-DFCP1 and immunolabeled with anti-Ub. Scale bar: 10 µm. (**e**) Quantification of VMP1 dots per cell associated with DFCP1, Ubiquitin or Ubiquitin and DFCP1. The graphic shows means and SEMs. N=10 cells in three independent experiments. (**f**) HeLa cells were transfected with VMP1-DsRed, LAMP1-YFPs and immunolabeled with anti-Ub. Scale bar: 10 µm. (**g**) Quantification of VMP1 dots per cell associated with Ubiquitin, Lysosome-associated membrane glycoprotein 1 (LAMP1) and Ub-LAMP1. The graphic shows means and SEMs. N=10 cells in three independent experiments. YFP: Yellow Fluorescent Protein.

We next studied if VMP1 remains ubiquitinated in the advanced steps of autophagy. By immunolabeling of LAMP2 (a lysosome marker) in VMP1-GFP transfected cells we found that VMP1 significantly colocalized with lysosomes labeled with LAMP2 (Figure 5A-B). Moreover, in cells concomitantly transfected with VMP1-DsRed and LAMP1-YFP, and immunolabeled with anti-LC3, we found that VMP1 co-distributed with LAMP1 and LC3, (Figure 5C-D). In addition, VMP1-DsRed and GFP-DFCP1 transfected cells, that were labeled with lysotracker, showed that the most of the VMP1 dots that are associated with lysosomal structures are not concomitantly associated with the omegasome (Figure 5E-F). These results suggest that VMP1 is present in the autolysosome. Finally, VMP1-DsRed and LAMP1-YFP co-transfected cells were immunolabeled with anti-ubiquitin. Figures 4F-G show that VMP1 present in the autolysosome is ubiquitinated, since 98% of VMP1 dots that co-distributes with LAMP1 are associated with ubiquitin dots (VMP1-Ub-Lamp1). These results demonstrate that VMP1 remains ubiquitinated in the autophagosome membrane after the fusion between the autophagosome and the lysosome.

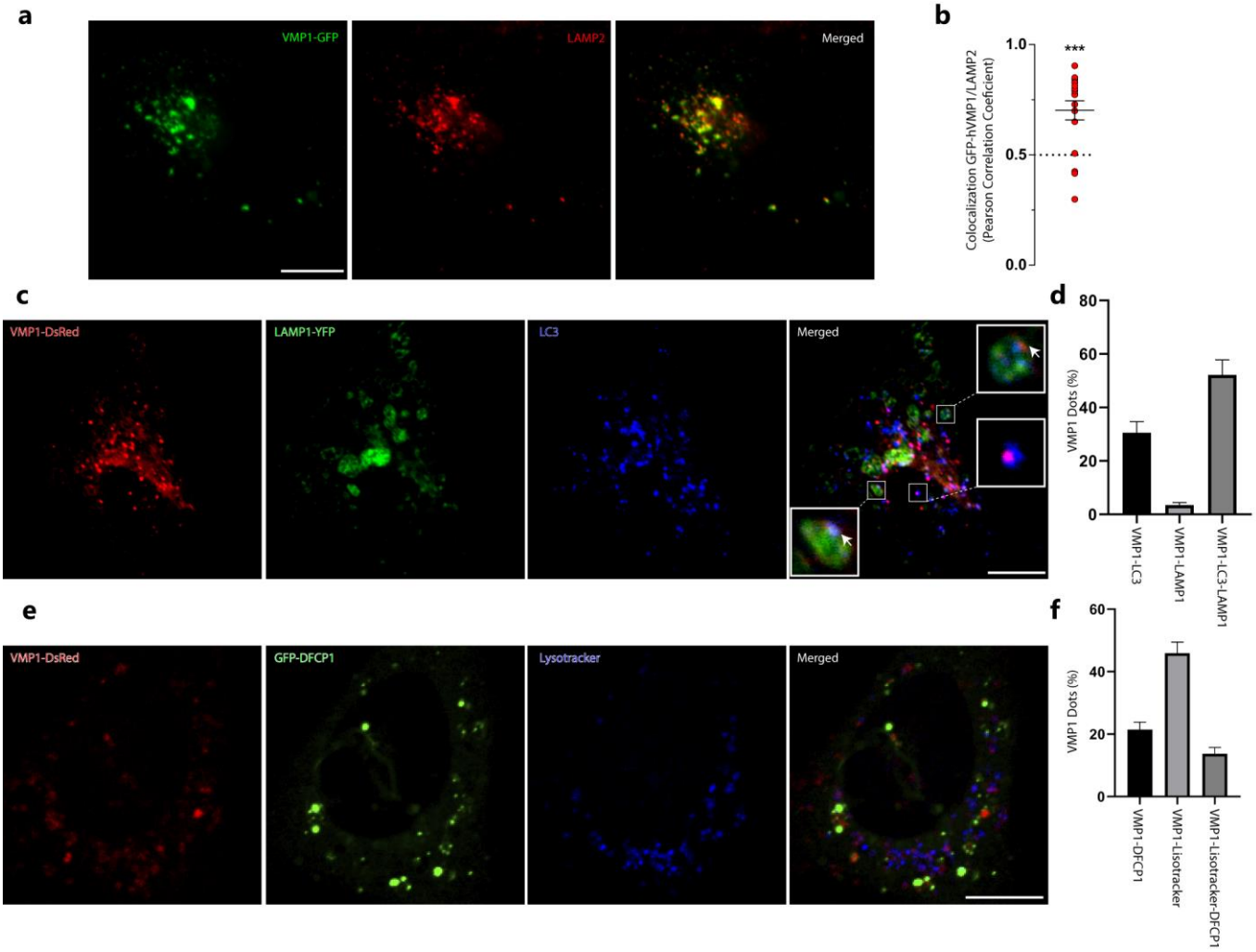

Figure 5. VMP1 remains ubiquitinated in the autophagic flux until autolysosome. (**a**) HEK293T cells were transfected with VMP1-GFP and immunolabeled with anti-LAMP2. Scale bars: 10 µm. (**b**) Colocalization between VMP1 and Lysosome-associated membrane glycoprotein 2 (LAMP2) was quantified by Pearson's Correlation Coefficient (PCC). Similar results were obtained in three independent experiments. Red plots show PCC for individual cells. n=17. ***: $p<0.001$ by Kruskall-Wallis test. (**c**) HeLa cells were transfected with VMP1-DsRed, LAMP1-YFPs and immunolabeled with anti-LC3. Scale bar: 10 µm. (**d**) Quantification of VMP1 dots per cell associated with LC3, LAMP1 and LC3-LAMP1. The graphic shows means and SEMs. N=10 cells in three independent experiments. (**e**) HeLaremain cells were transfected with VMP1-DsRed, GFP-DFCP1 and labeled with Lysotracker Blue DND-22. Scale bar: 10 µm. (**f**) The graphic shows means and SEMs of VMP1 dots associated with DFCP1, Lysotracker, or DFCP1 and Lysotracker. N=10 cells in three independent experiments.

2.4. The E3 ligase complex CRL4/Cdt2 is involved in the ubiquitination of VMP1

The cullin-RING E3 ubiquitin ligase CRL4/Cdt2 is known for being a main modulator of genome stability, targeting important cell cycle proteins for degradation, as the CDK inhibitor p21 and the Chromatin Licensing and DNA Replication Factor 1 (Cdt1) [27]. A schematic representation of this complex is shown in Figure 6A, where we can see the protein Cdt2 working as the substrate recognition subunit through direct binding to the protein to be ubiquitinated. Although the role of Cdt2 as a regulator of the cell cycle has been widely studied, little is known about extra-nuclear possible roles. To find new CRL4/Cdt2 substrates, HEK 293T cells were transfected with FLAG-HA-Cdt2, where Cdt2 was purified by tandem affinity purification from soluble and chromatin-

linked fractions. These fractions were separated and independently analyzed by the Mass spectrometry approach. Conspicuously, VMP1 was found as a new Cdt2 interactor in the soluble fraction, but not in the chromatin-linked one (Figure 6B). To confirm the Cdt2-VMP1 interaction, we performed immunoprecipitation with anti-FLAG in VMP1-FLAG and Myc-Cdt2 transfected cells. We found Myc-Cdt2 in the eluates indicating the VMP1-Cdt2 interaction (Figure 6C). Moreover, we found endogenous VMP1 in eluates from FLAG-Cdt2 transfected cells immunoprecipitated with anti-FLAG (Figure 6D), confirming the interaction between these two proteins.

Given the essential cell cycle regulatory function of Cdt2, it is not a surprise that it is mainly localized in the nucleus. Since the high colocalization found between VMP1 and Ub has place mainly in the cell cytoplasm, we hypothesized that if Cdt2 participates in the VMP1 ubiquitination, a fraction of Cdt2 should be translocate to the extranuclear region when VMP1-GFP is expressed. To test this hypothesis, we performed immunofluorescence with anti-FLAG in FLAG-Cdt2 transfected cells in presence or absence of VMP1-EGFP transfection. While cells without VMP1-GFP transfection showed a mainly nuclear Cdt2 localization, cells with VMP1-GFP showed extranuclear localization and co-distribution between VMP1 and Cdt2 in the cytoplasm (Figure S3). We then performed immunofluorescence to detect endogenous Cdt2 in cells with or without VMP1-GFP expression and the translocation of Cdt2 under VMP1 expression was confirmed. While cells without VMP1-GFP transfection showed mainly nuclear localization of Cdt2 (Figure 6E), cells expressing VMP1-GFP showed mainly extranuclear localization of Cdt2 (Figure 6F). This last observation was quantified measuring the integrated fluorescence signal intra and extranuclear. The ratio of extranuclear/nuclear signal was increased significantly in cells expressing VMP1-GFP (Figure 6G). Taken together, these results indicate that VMP1 interacts with Cdt2 and suggest that the ubiquitin ligase CRL4/Cdt2 might catalyze the ubiquitination of VMP1. To test if VMP1-Cdt2 interaction might be involved in the ubiquitination of VMP1, we overexpressed FLAG-Cdt2 in cells co-expressing VMP1-GFP and Myc-Ub. The lysates of these cells were immunoprecipitated with Anti-Myc linked to Protein G – Sepharose. In the immunoblot with Anti-GFP we observed that the ubiquitinated VMP1 increased under FLAG-Cdt2 overexpression (Figure 6H). Finally, we performed the IP of Myc-Ub in VMP1-GFP transfected cells treated with MLN4924. MLN4924 is a neddylation inhibitor that avoids the CRL E3 Ligases activation [28]. We found that the VMP1 ubiquitination decreases in presence of the CRL ligases inhibitor (Figure 6H). Taken together, these results indicate that VMP1 interacts with Cdt2 and suggest that the ubiquitin ligase CRL4/Cdt2 can catalyze the ubiquitination of VMP1. Moreover, by fluorescence microscopy we observed that the treatment with MLN4924 in VMP1-GFP transfected cells affects the characteristic recruitment of VMP1, decreasing significantly the VMP1 dots per cell (Figure 6I-J). This last finding suggests that ubiquitinated VMP1 is involved in VMP1-mediated autophagy.

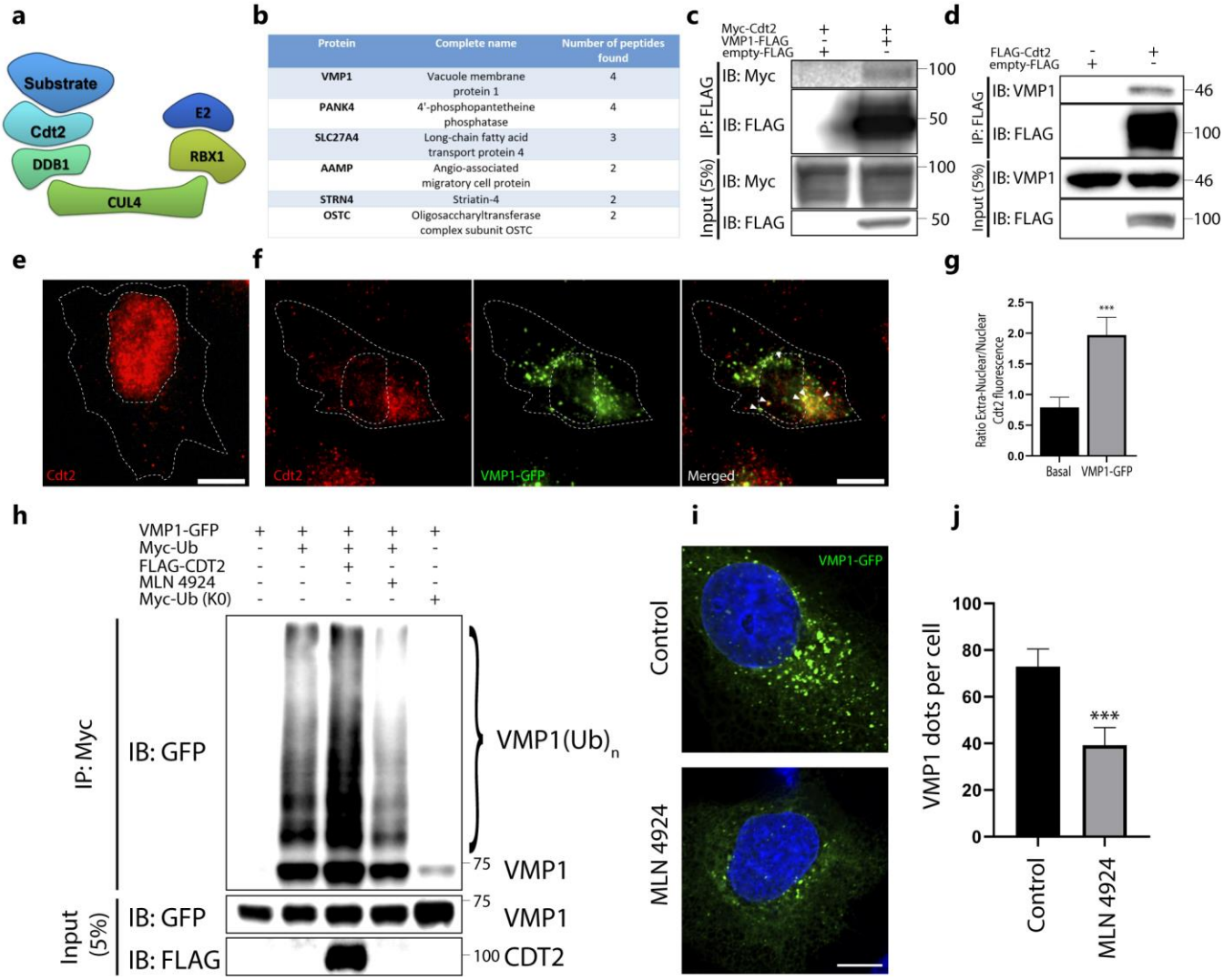

Figure 6. Cdt2 is involved in the ubiquitination of VMP1. (**a**) Schematic representation of the E3 ligase complex Cullin–RING ubiquitin ligase complex 4 (CRL4)/Cdt2, in which the Cell division cycle protein cdt2 (Cdt2) works as the substrate recognition subunit. (**b**) Table of main interactors of Cdt2 founded by MS of the sequential immunoprecipitation with anti-FLAG and anti-HA of soluble fraction (non-chromatin fraction) HEK293T cells transfected with FLAG-HA-Cdt2. VMP1 was found between the interactors. (**c**) Lysates from HEK293T cells transfected with Myc-Cdt2 and VMP1-FLAG were immunoprecipitated with anti-FLAG magnetic beads and immunoblotted with anti-Myc. (**d**) Lysates from HEK293T cells transfected with FLAG-Cdt2 were immunoprecipitated with anti-FLAG magnetic beads and immunoblotted with anti-VMP1. (**e**) HeLa cells were immunolabeled with anti-Cdt2. Scale bar: 10 µm. (**f**) HeLa cells were transfected with VMP1-GFP and immunolabeled with anti-Cdt2. Scale bar: 10 µm. (**g**) Endogenous Cdt2 localization was measured as the ratio between extra-nuclear and intra-nuclear integrated density of fluorescence in VMP1-GFP and non-transfected HeLa cells. ***p<0.001 vs control by Mann-Whitney nonparametric test. (**h**) Lysates from HEK293T cells transfected with VMP1-GFP and Myc-Ub with or without Cdt2-FLAG and treated or not with MLN4924 (0,5 µM, 5h), were immunoprecipitated with anti-Myc linked to Protein G – Sepharose. The eluates were immunoblotted with anti-GFP. Ubiquitinated VMP1 increases in presence of Cdt2-FLAG and decreases under treatment with MLN4924. Myc-Ub (K0) has been used as a negative control. The images are representative of three independent experiments. (**i**) HeLa cells were immunolabeled with pLenti-VMP1-GFP and treated with or not with MLN4924 (0,5 µM, 5h). Scale bar: 10 µm. (**j**) Quantification of VMP1 dots per cell in control and MLN 4924 treated cells. The graphic shows means and SEMs. N=18 control cells and 22 MLN 4924 treated cells in three independent experiments. ***: p<0.001 vs Control by Mann Whitney test.

3. Discussion

Autophagy is an essential catabolic process, which is fundamental for cellular homeostasis maintenance. Dysfunctional autophagy is directly related to pathologic occurrence. Diabetes, cardiovascular diseases, neurodegenerative disorders, and cancer have been linked to autophagy alterations as part of their pathophysiological mechanisms [29]. Regarding cancer, a large set of data showed a complex and contradictory role of autophagy in the progression of the disease. In early stages, autophagy plays a protective role, in which it avoids the accumulation of damaged cellular components and enhances immunosurveillance, contributing to tumor suppression. However, in advanced cancers, autophagy acts to promote tumor survival and growth, helping to cope with adverse conditions such as hypoxia and nutritional deficiency [30]. Indeed, several studies have demonstrated an important role of autophagy in chemotherapy resistance [31]. Previously we found that the expression of the transmembrane protein VMP1 triggers autophagy in human tumor cells [24]. VMP1-mediated autophagy is induced by gemcitabine through the transcription factor E2F1 in pancreatic cancer cells and by photodynamic therapy through HIF-1α in colon cancer cells. Both pathways of VMP1 transcriptional regulation

promote tumor cell resistance to anticancer treatment [22,25]. In this work, we focus on posttranslational regulation of VMP1 by Ubiquitin system, which is highly implicated in the regulation of metabolic reprogramming in cancer cells [32]. In addition, ubiquitination plays an important role in modulating autophagy and managing this regulatory mechanism could be of relevance for cancer therapy. We have identified ubiquitination as a novel post translational modification of the autophagy related transmembrane protein VMP1. Our results indicate that VMP1 is ubiquitinated in the early steps of autophagosome biogenesis and remains ubiquitinated as part of the autophagosome membrane throughout the autophagic flux until autolysosome formation. Moreover, we have shown that the E3 ligase substrate adaptor Cdt2, whose action is closely related to the cell cycle regulation [33], is a new partner of VMP1 and is involved in VMP1 ubiquitination.

We have shown that VMP1 is modified by ubiquitination using immunofluorescence and immunoprecipitation techniques (Figure 1). In the immunoprecipitation of FLAG-Ub (Figure 1E) we confirmed that VMP1 is ubiquitinated, since several bands upper the VMP1-GFP molecular weight can be found in the immunoblot with anti-VMP1. Considering that the theoretical molecular weight for VMP1-GFP is 73,2 kDa and FLAG-Ub is 9,8 kDa, the band around 85 kDa that is also present in the immunoblot, could mean mono-ubiquitination of VMP1, which theoretical MW would be 83 kDa. However, when we investigated monoubiquitination in Figure 2B we did not find ubiquitination of VMP1 with the Myc-Ub (K0), a ubiquitin molecule that is unable to form ubiquitin chains. Therefore, we conclude that VMP1 is polyubiquitinated but not monoubiquitinated. In this way, the 85kDa band in Figure 1F might represent the first ubiquitin molecule in the polyubiquitination chain.

Immunofluorescence and immunoprecipitation assays, using diverse expression systems for VMP1, showed that VMP1 is ubiquitinated as soon as it is expressed (Figure 1). However, ubiquitination would not lead to the degradation of VMP1. Indeed, it was not accumulated after proteasomes or lysosomes were blocked. Therefore, early ubiquitination of VMP1 might not explain VMP1 degradation by ubiquitin-proteasome system or by autophagy (Figure 3). Since ubiquitinated VMP1 is not broken down by autophagosomes or the proteasome system, it is important to note that certain deubiquitinases could be involved in the retrieval of non-ubiquitinated VMP1. In fact, we have previously found that the deubiquitinase Probable ubiquitin carboxyl-terminal hydrolase FAF-X (USP9x) is an interactor of VMP1 in the context of the selective autophagy of zymogen granules during experimental acute pancreatitis [17]. On the other hand, under the inhibition of the autophagic flux (Figure 3H-J), a small but significant decrease in VMP1-GFP was found. This could be affected by translational regulation feedback in response to the inhibition of the autophagic flux. Given VMP1 expression is triggered under acute stress conditions [12,13], a rapid regulation at mRNA level is also feasible. In this way, under CHX treatment, we did not find changes between the CQ treated and untreated cells. These findings show that the reduction of VMP1 levels after CQ inhibition only occurs when the translation is active, endorsing the hypothesis of a translational regulation feedback. According to our results, VMP1 is not a cargo of autophagy. This observation is consistent with the results shown by Itakura & Mizushima [34] where only a few dots formed by the cargo receptor p62 colocalize with VMP1-GFP dots. Notably, after 16 h of CHX treatment we found an important decrease in VMP1 levels, but this reduction was not avoided by CQ nor MG132 treatments. Recent reports demonstrated that some autophagy-related proteins and cargo molecules are plausible to be eliminated by secretory pathways [35,36]. Further studies would be necessary to fully elucidate VMP1 degradation mechanisms.

In this work we have demonstrated that VMP1 is ubiquitinated when it is involved in the autophagic process (Figure 4). Ubiquitinated VMP1 is associated to a significant LC3 recruitment (Figure 4A-C). Interestingly, we noted that, although most of the VMP1 is ubiquitinated (Figure 4C), there is a little portion that is not. This portion of non-ubiquitinated VMP1 is located principally in the perinuclear region (Figure 4A) and is poorly distributed with LC3 (Figure 4C). Therefore, it is proposed that only the ubiquitinated VMP1 would participate in autophagosome biogenesis. Indeed, in Figure 4D-E we show that VMP1 is ubiquitinated when it co-distributes with the omegasome marker DFCP1.

We have previously demonstrated that VMP1 is a transmembrane protein in the autophagosome [17,18]. However, no data about the presence or absence of VMP1 in the autolysosome has been reported up to now. In this work, we have found significant colocalization between VMP1 and the lysosome marker LAMP2 (Figure 5A-B). Moreover, a triple association between VMP1, LAMP1 and LC3 has been found (Figure 5C-D), suggesting that VMP1 is present in the autophagosomal membrane throughout the autophagic flux. Indeed, when we investigated the proportion of VMP1 associated to lysosomes we found that most of the VMP1 dots associated with lysosomes were not concomitantly associated with omegasomes (Figure 5E-F). These findings show for the first time that VMP1 is not only present in the autophagosome but also remains as a transmembrane protein of the autophagosome until its fusion with the lysosome. Importantly, we found a triple co-distribution between VMP1, LAMP1 and Ub (Figure 4F-G), indicating that VMP1 remains ubiquitinated when it arrives at the autolysosome.

Ubiquitination plays an essential role in autophagy regulation since most of a long list of autophagy-related proteins are regulated by ubiquitination [5]. For instance, under poor nutrient conditions, Unc-51-like kinase 1 (ULK1) is modified by the E3 ligase TNF receptor (TNFR)-associated factor 6 (TRAF6) enhancing its stability and function [37]. In the PI3KC3 Complex 1, Vps34 and ATG14 ubiquitination leads to proteasome degradation [38,39]. BECN1 is K63 polyubiquitinated, allowing its autophagy recruitment [40] or K11 and K48 polyubiquitinated for proteasomal degradation [41,42]. WIPI2 ubiquitination leads to its proteasomal degradation, and it is mediated by the Cul4 family of ubiquitin ligase during mitosis [43]. Here we have analyzed VMP1 ubiquitination as a complete set; it would be possible that more than one VMP1 ubiquitination site and different types of ubiquitination of VMP1 occur, and these modifications might regulate VMP1 functions. It is important to note that in this work we used overexpressed VMP1 to simplify the study of VMP1 ubiquitination. Further studies will be necessary to know about how this modification intervenes in a physiological and/or pathological context and how it could be modulated.

Furthermore, we found that Cdt2 is a new VMP1 interactor (Figure 6 B-D). Cdt2 works as the substrate recognition factor in the E3 ligase complex CRL4/Cdt2 [34,45]. The interaction between Cdt2 and VMP1 points at this E3 ligase as an important candidate to catalyze the ubiquitination of VMP1. So far it is known that the complex CRL4/Cdt2 plays a fundamental role in the regulation of genome stability. CRL4/Cdt2 labels important cellular substrates for proteasomal degradation during S phase of the cell cycle. Some of the known substrates of CRL4/Cdt2 are Cdt1, the CDK inhibitor p21 and the histone methyltransferase Set8 (KMT5A). All of them are key regulators of DNA replication and its degradation prevents the re-replication [27,33]. In the mass spectrometry performed in this work, we separated two fractions, the soluble fraction, and the chromatin-attached fraction. VMP1 has been found to be the main interactor present in the soluble fraction, but it is not present in the chromatin-attached fraction. Probably it implies a novel function for Cdt2, given that the main described interactors up to now, have been nuclear proteins. We indeed demonstrated that the overexpression of VMP1 triggers Cdt2 relocation (Figure 6 E-G and Figure S3) and an important part of Cdt2 seems to leave the nucleus to interact with VMP1 when VMP1 is overexpressed. The translocation of Cdt2 is a totally novel event that supports our findings that VMP1 is regulated by ubiquitination as soon as it is expressed. In addition, we demonstrated that Cdt2 is involved in the VMP1 ubiquitination, since Cdt2 overexpression increases the ubiquitination of VMP1, and the CRLs inhibition by MLN4924 drives to a decrease in VMP1 ubiquitination (Figure 6H). Finally, although MLN4924 could exert indirect effects, the finding that VMP1 subcellular localization is affected under MLN4924 treatment (Figure 6I-J) suggests that VMP1 ubiquitination is necessary for VMP1-mediated autophagy.

It is very interesting to note that both VMP1 and Cdt2 play important roles in tumor resistance. While VMP1 has been related with poor patient outcome in pancreatic [21] and breast cancer [44], Cdt2 has been associated with more aggressiveness of hepatocellular carcinoma [45], gastric cancer [46] and melanoma [47]. Moreover, in pancreatic cancer, the inhibition of the CRL E3 ligases with MLN4924, has shown to increase the sensibility to radiotherapy [48]. Therefore, it is possible that VMP1 and CRL4 molecular pathways might be cross talking during tumor progression.

4. Materials and Methods

4.1 Cell Culture and Transfections

HEK293T, HeLa, PANC-1 and MCF-7 cell lines were obtained from the American Type Culture Collection (ATCC). These cell lines were cultured in Dulbecco's modified Eagle's medium (Biological Industries) supplemented with 10% fetal bovine serum (Natocor), L-alanyl-L-glutamine dipeptide 200 mM (Gibco™), 100 U µl−1 penicillin, and 100 µg µl−1 streptomycin (Biological Industries). The cell lines were maintained at 37°C and 5% CO2 under a humidified atmosphere. Mycoplasma contamination is checked monthly by DAPI staining and by PCR every six months. Transfections were performed using X-treme GENE 9 DNA transfection reagent (Roche Applied Science) according to the manufacturer's instructions.

4.2 Treatments

For amino-acid starvation, cells were washed two times with starvation medium (140 mM NaCl, 1 mM CaCl2, 1 mM MgCl2, 5 mM glucose, 1% BSA and 20 mM HEPES pH 7.4), and incubated with the same starvation medium for 1 h. Pp242 (Santa Cruz) was dissolved in DMSO in a 1mM stock solution and applied during 1h in a 1 µM final concentration. Chloroquine diphosphate salt (Sigma Aldrich) was dissolved in PBS in a 10 mM stock and applied during 16 or 24 h in a 50 µM final concentration, or during 2 to 8 h in a 100 50 µM concentration. MG132 (PeptaNova) was dissolved in DMSO in a 10 mM stock solution and applied during 6h in a 10µM final concentration. Cycloheximide (CHX) (Sigma-Aldrich), was applied during 2, 4, 6, 8 or 16 h in a 100 µg/mL concentration. MLN4924 (Selleckchem) was dissolved in DMSO in a 0,5mM stock solution and was applied during 5h in a 5µM concentration.

4.3 Expression Vectors

The plasmid pEGFP-N1-VMP1 was performed inserting the human VMP1 sequence (NCBI Reference Sequence: NM_030938.5) into the pEGFP-N1 (CLONTECH cat. #6085-1). The plasmid pcDNA4-B-hVMP1-V5/His was performed inserting the human VMP1 sequence (NM_030938.5) into the pcDNATM4/V5-HisB (Invitrogen Catalog number V861-20). pcDNA4-B-hVMP1-V5/His was performed inserting the human VMP1 sequence (NM_030938.5) into the pcDNATM4/V5-HisB (Invitrogen Catalog number V861-20). pLenti-hVMP1-flag was performed inserting the oligonucleotide MCS-flag into the pENTR1A (Addgene Plasmid #17398). The new vector was named pENTR1F-flag2. Human VMP1 sequence (NM_030938.5) was cloned into pENTR1F-flag2 using the GatewayTM LR ClonaseTM II (cat n# 11791-020). pLVX-DsRed-Monomer-N1-hVMP1 was performed inserting the human VMP1 sequence (NCBI Reference Sequence: NM_030938.5) into the pLVX-DsRed-Monomer-N1 (CLONTECH cat. 632152). pLenti-VMP1-GFP was performed through cloning VMP1 sequence (NCBI Reference Sequence: NM_030938.5) into pENTR1A-GFP-N2 (FR1) (Addgene Plasmid #19364). The new vector was recombined with pLenti PGK puro (Addgene Plasmid #19068). LAMP1-YFP and GFP-DFCP1 were obtained from Addgene (Plasmid #1816, 38269). FLAG-Ub has been kindly gifted from Simona Polo (University of Milan). The plasmids pWC7-His-Myc-Ubiquitin wt and pWC7-His-Myc-Ubiquitin Kless were kindly gifted from Daniele Guarvaccaro (University of Verona). The plasmid pcDNA3-2xFLAG-2xHA-Cdt2 was performed as previously reported [49]. The plasmid pcDNA3-Myc-Cdt2 was performed inserting the human Cdt2 cDNA sequence in the pcDNA3.1 vector.

4.4 Western Blot Analysis

After different treatments and transfections, cells were lysed in lysis buffer (50 mM Tris-HCl pH 7.4, 250 mM NaCl, 25 mM NaF, 2mM EDTA, 0.1% Triton X-100 and Thermo Scientific™ Pierce Protease Inhibitors). For LC3 western blots cells were lysed in 50 mM Tris-HCl pH 8.0, 150 mM NaCl, 1% Triton X-100 and Thermo Scientific™ Pierce Protease Inhibitors. Protein concentration was determined using the bicinchoninic acid (BCA) protein assay reagent (Pierce). An equal amount of protein was analyzed on SDS-PAGE and transferred to polyvinylidene fluoride PVDF membranes (0.22 µm pore size, Millipore). The membranes were blocked with Odyssey Blocking Buffer (LI-COR) at room temperature for 1 h and incubated with the corresponding primary antibodies overnight at 4°C. The primary antibodies used were anti-VMP1 (1:1,000; rabbit mAb #12978, Cell Signaling Technology), anti-Actin (1:2,000; rabbit polyAb A2066; Sigma–Aldrich), anti-Ubiquitin (1:1000; mouse mAb UBCJ2; Enzo), Anti-DYKDDDDK Tag (1:6000; mouse mAb #8146, Cell Signaling Technology),anti α-Tubulin (1:4000; mouse mAb T5168; Sigma-Aldrich)anti-Myc (1/1000; rabbit polyclonal ab9106; ABCAM) and anti-GFP (1/3000, Rabbit pAb TP401, Torrey Pines Biolab). After incubation, the membrane was washed four times with PBS containing 0.1% Tween-20 (PBS-T), twice with PBS, and then incubated with the corresponding IRDye secondary antibody (1:15000, IRDye® 680LT Goat anti-Rabbit IgG or 1:10000, IRDye® 800CW Goat anti-Mouse IgG, LI-COR) in Odyssey Blocking Buffer (LI-COR) for 2 h at room temperature. Finally, the membrane was washed four times with PBST, twice with PBS, and scanned with Odyssey® SA (LI-COR).

For the LC3 western blotting, membranes were blocked at room temperature for 1 h with 1% Bovine Serum Albumin in TRIS-buffered saline (TBS) containing 0.1% Tween-20 (TBS-T). After blocking, membranes were incubated with the primary antibody anti-LC3B (1:500, Rabbit mAb #3868, Cell Signaling Technology) during 24h at 4°C. After the incubation, the membranes were washed four times with TBS-T and twice with TBS. Finally, they were incubated with anti-rabbit HRP-conjugated (1:2500, Amersham NA934, GE Healthcare) secondary antibody in 1% Bovine Serum Albumin in TRIS-buffered saline (TBS) containing 0.1% Tween-20 (TBS-T). The membranes were washed four times with TBST, twice with TBS and incubated with PIERCE ELC Plus Western blotting Substrate (Cat# 32134, Thermo Scientific) according to manufacturer's instructions and scanned with cDigit Blot Scanner (LI-COR).

FIJI software has been used to determine the protein bands density. Relative densitometry normalized to actin, is expressed as the mean ± SEM of three different experiments.

4.5 Immunoprecipitation Assays

For Anti-FLAG immunoprecipitations, supernatants of lysed cells were incubated in shake tubes during 2h at 4ºC with Anti-FLAG® M2 Magnetic Beads. The Beads were washed with lysis buffer and eluates were performed by addition of Laemmli Buffer.

For Anti-V5 immunoprecipitations, supernatants of lysed cells were incubated in shake tubes during 1h at 4ºC with Pierce™ Protein G Magnetic Beads (Invitrogen) previously attached to V5 Tag Antibody (R960-25). The Beads were washed with lysis buffer and eluates were performed by addition of Laemmli Buffer.

For Anti-Myc immunoprecipitations, supernatants of lysed cells were incubated in shake tubes during 16h at 4ºC c-Myc Antibody (9E10 M5546, Merck). Then, the lysates were incubated in shake tubes during 1h at 4ºC with Recombinat Protein G Sepharose (Invitrogen). The Sepharose was washed with RIPA lysis buffer and eluates were performed by addition of Laemmli Buffer.

4.6 Mass Spectrometry

HEK293T cells were transfected with Flag-HA tagged Cdt2 (CDT2) or the Empty Vector (PCDNA). CSK soluble fraction and Chromatin cell extracts were subjected to immunoprecipitation with an anti-Flag antibody and eluted by competing with Flag peptide. Then, the material was immunoprecipitated with an anti-HA antibody. Mass spectrometry approach was used to identify new CRL4/Cdt2 substrates.

4.7 Immunofluorescence

For Hela, PANC-1 and MCF-7 cells, the following protocol was applied: The cells were growing on 12 mm round glass coverslips into 24-well-plates. 3.5x104 HeLa, 5x104 MCF-7 or 2.5x104 PANC-1 were seeded. The next day (or two days in the case of PANC-1), cells were transfected. After 24h, they were treated, fixed with 3.6 % p-formaldehyde for 20 minutes, permeabilized for 5 minutes in Triton 0.1 % in PBS and blocked during 1h. Glasses were incubated overnight with the primary antibody at 4°C. The used antibodies were anti-Ubiquitin (1:2000, mouse mAb UBCJ2; Enzo), Anti-LC3 (1:1000, Rabbit mAb #3868, Cell Signaling Technology), Anti-FLAG (1:500; DYKDDDDK Tag (9A3) Mouse mAb; Cell Signaling Technology) and anti-Cdt2 (1:1000; Rabbit polyclonal antibody NB100-40840; Novus Biologicals). Next day, glasses were incubated for 2h at room temperature with secondary antibodies (1:800 Alexa Fluor 594 and 647 antibodies from Molecular Probes) and mounted in Polyvinyl alcohol mounting medium with DABCO. For lysotracker staining, the cells were incubated during 45 minutes with LysoTracker™ Blue DND-22 160 nM (Thermo Fisher) and immediately seen and photographed in the confocal microscopy in absence of fixation.

For HEK 293T cells, 80% confluency cells were transfected in a 6-well. The next day, they were seeded on 16 mm round glass coverslips into 12-well plates. After 24h, they were treated, fixed with 3,6 % p-formaldehyde in PBS for 20 minutes, permeabilized with NETgel (150 mM NaCl, 5 mM EDTA, 50 mM Tris Cl, pH 7.4, 0.05% (v/v) NP-40, 0.25% (w/v), gelatin (from bovine skin; Sigma, cat. no. G-6650) and 0.02% (w/v) sodium azide) containing 0.25% NP40 and stained for 30 min with the primary antibody. The antibodies used were anti-Ub (1:100; mouse monoclonal antibody FK2; ENZO), anti-LAMP2 (1:100; mouse monoclonal antibody; Developmental Studies Hybridoma Data Bank) and anti-ATG13 (1:100, mouse monoclonal antibody MABC46; Millipore). After the primary antibody incubation, the cells were washed 3 times during 5 minutes with NETgel and stained for 30

min with Goat anti-Mouse IgG - Alexa Fluor 568. Mountage was performed with Aqua Poly Mount mounting medium (Polysciences, cat. no. 18606).

The sample observation and images acquisition were performed in a a Zeiss Axio Imager D2 wide-field epi-fluorescence microscope equipped with a 63 1.4 NA lens, AxioCam HR CCD camera (Zeiss) and HXP 120C metal halide light source (Zeiss) and an inverted LSM Olympus FV-1000 using an UPLSAPO 60X O NA: 1.35 objective.

4.8 Quantification of colocalization

Pearson's correlation coefficient for the selected ROI corresponding to the cell of interest was quantified using the plugin EzColocalization in Fiji (Fiji Is Just ImageJ) Open-Source software.

4.9 Quantification of puncta per cell

The number of puncta per cell was obtained through the 3D objects counter tool in Fiji (Fiji Is Just ImageJ) Open-Source software.

4.10 Quantification of dots association

The images of HeLa transfected with VMP1-GFP and immunolabeled with anti-LC3 and anti-Ubiquitin (with or without PP242 treatment) were analyzed using Fiji (Fiji Is Just ImageJ) Open-Source software. For the study of the association between LC3 or VMP1 and the other labelled proteins, we draw a 5 µm2 per point grid over the composite image. For each LC3 or VMP1 point, the association with the signals in the other channels were judged using a large magnification.

4.11 Quantification of Ratio Extra-nuclear/Nuclear localization

Using Fiji (Fiji Is Just ImageJ), we designed two ROIs per cell. The first one was performed rounding the nucleus, and the second one, rounding the complete cell but excluding the nucleus. Integrated density was measured for each ROI and the ratio between the extranuclear / nuclear measurement was calculated.

4.12 Statistical Analysis

Data are expressed as mean ± SEM. All the shown images are representative of three independent experiments. Statistical analysis of data was performed using GraphPad Prism 8 as stated in corresponding figures legends.

5. Conclusions

In the present study we have identified ubiquitination as a posttranslational modification for VMP1. The VMP1 ubiquitination does not lead to degradation by the autophagy or the ubiquitin-proteasomal system. Moreover, we demonstrated that VMP1 is ubiquitinated early in autophagosome biogenesis and remains ubiquitinated as part of the autophagosome membrane throughout autophagic flux. Finally, VMP1 interacts with Cdt2, the substrate recognition subunit of the CRL4/Cdt2 E3 ligase complex, which is involved in the ubiquitination of VMP1 (Figure 7). We conclude that ubiquitination is a novel posttranslational modification of VMP1 in the context of VMP1-mediated autophagy of human tumor cells and might have clinical relevance in cancer cells resistance to therapy.

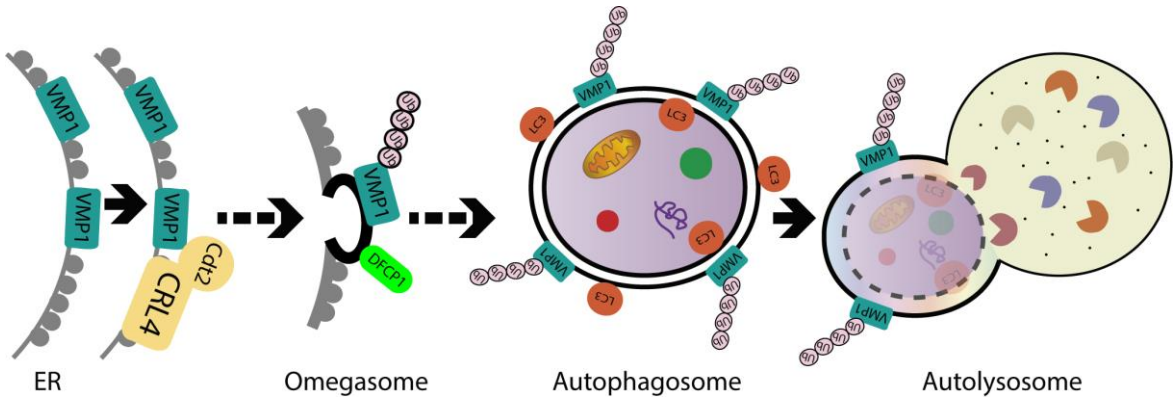

Figure 7. Schematic model. VMP1 is ubiquitinated since the initial steps of autophagosome biogenesis and remains ubiquitinated throughout the autophagic flux till autolysosome formation. Moreover, VMP1 interacts with Cdt2, the adaptor subunit of the CRL4/Cdt2 E3 ligase complex, that is able to catalyze the VMP1 ubiquitination. ER: Endoplasmic reticulum.

Funding: This work was supported by grants from: Consejo Nacional de Investigaciones Científicas y Técnicas (CONICET) [PIP 2021-2023 GI− 11220200101549CO; and PUE 22920170100033]; Agencia Nacional de Promoción Científica y Tecnológica (ANPCyT) [PICT2019- 01664] and Universidad de Buenos Aires [UBACYT 2018-2020 20020170100082BA].

Conflicts of Interest: The authors declare no conflict of interest.

Acknowledgments: Authors would like to thank the Vaccaro's lab members for their contributions in the discussion of results and the laboratory's quality ensure system. We are grateful to Guido Petrovich, Victoria Mestre Cordero and Gregorio McCallum for their help in methodologic issues.

References

1. Ktistakis, N.T.; Tooze, S.A. Digesting the Expanding Mechanisms of Autophagy. *Trends Cell Biol* **2016**, *26*, 624-635, doi:10.1016/j.tcb.2016.03.006.
2. Grasso, D.; Renna, F.J.; Vaccaro, M.I. Initial Steps in Mammalian Autophagosome Biogenesis. *Front Cell Dev Biol* **2018**, *6*, 146, doi:10.3389/fcell.2018.00146.
3. Yang, Z.; Klionsky, D.J. Mammalian autophagy: core molecular machinery and signaling regulation. *Curr Opin Cell Biol* **2010**, *22*, 124-131, doi:10.1016/j.ceb.2009.11.014.
4. Wani, W.Y.; Boyer-Guittaut, M.; Dodson, M.; Chatham, J.; Darley-Usmar, V.; Zhang, J. Regulation of autophagy by protein post-translational modification. *Lab Invest* **2015**, *95*, 14-25, doi:10.1038/labinvest.2014.131.
5. Chen, R.H.; Chen, Y.H.; Huang, T.Y. Ubiquitin-mediated regulation of autophagy. *J Biomed Sci* **2019**, *26*, 80, doi:10.1186/s12929-019-0569-y.
6. Noda, N.N.; Fujioka, Y. Atg1 family kinases in autophagy initiation. *Cell Mol Life Sci* **2015**, *72*, 3083-3096, doi:10.1007/s00018-015-1917-z.
7. Stjepanovic, G.; Baskaran, S.; Lin, M.G.; Hurley, J.H. Unveiling the role of VPS34 kinase domain dynamics in regulation of the autophagic PI3K complex. *Mol Cell Oncol* **2017**, *4*, e1367873, doi:10.1080/23723556.2017.1367873.
8. Gutierrez, M.G.; Munafo, D.B.; Beron, W.; Colombo, M.I. Rab7 is required for the normal progression of the autophagic pathway in mammalian cells. *J Cell Sci* **2004**, *117*, 2687-2697, doi:10.1242/jcs.01114.
9. Jiang, P.; Nishimura, T.; Sakamaki, Y.; Itakura, E.; Hatta, T.; Natsume, T.; Mizushima, N. The HOPS complex mediates autophagosome-lysosome fusion through interaction with syntaxin 17. *Mol Biol Cell* **2014**, *25*, 1327-1337, doi:10.1091/mbc.E13-08-0447.
10. Hershko, A.; Ciechanover, A. The ubiquitin system. *Annu Rev Biochem* **1998**, *67*, 425-479, doi:10.1146/annurev.biochem.67.1.425.
11. Schulman, B.A. Twists and turns in ubiquitin-like protein conjugation cascades. *Protein Sci* **2011**, *20*, 1941-1954, doi:10.1002/pro.750.
12. Dusetti, N.J.; Jiang, Y.; Vaccaro, M.I.; Tomasini, R.; Azizi Samir, A.; Calvo, E.L.; Ropolo, A.; Fiedler, F.; Mallo, G.V.; Dagorn, J.C.; et al. Cloning and expression of the rat vacuole membrane protein 1 (VMP1), a new gene activated in pancreas with acute pancreatitis, which promotes vacuole formation. *Biochem Biophys Res Commun* **2002**, *290*, 641-649, doi:10.1006/bbrc.2001.6244.
13. Ropolo, A.; Grasso, D.; Pardo, R.; Sacchetti, M.L.; Archange, C.; Lo Re, A.; Seux, M.; Nowak, J.; Gonzalez, C.D.; Iovanna, J.L.; et al. The pancreatitis-induced vacuole membrane protein 1 triggers autophagy in mammalian cells. *J Biol Chem* **2007**, *282*, 37124-37133, doi:10.1074/jbc.M706956200.
14. Molejon, M.I.; Ropolo, A.; Re, A.L.; Boggio, V.; Vaccaro, M.I. The VMP1-Beclin 1 interaction regulates autophagy induction. *Sci Rep* **2013**, *3*, 1055, doi:10.1038/srep01055.

15. Nascimbeni, A.C.; Giordano, F.; Dupont, N.; Grasso, D.; Vaccaro, M.I.; Codogno, P.; Morel, E. ER-plasma membrane contact sites contribute to autophagosome biogenesis by regulation of local PI3P synthesis. *EMBO J* **2017**, *36*, 2018-2033, doi:10.15252/embj.201797006.
16. Zhao, Y.G.; Zhang, H. The ER-localized autophagy protein EPG-3/VMP1 regulates ER contacts with other organelles by modulating ATP2A/SERCA activity. *Autophagy* **2018**, *14*, 362-363, doi:10.1080/15548627.2017.1415591.
17. Grasso, D.; Ropolo, A.; Lo Re, A.; Boggio, V.; Molejon, M.I.; Iovanna, J.L.; Gonzalez, C.D.; Urrutia, R.; Vaccaro, M.I. Zymophagy, a novel selective autophagy pathway mediated by VMP1-USP9x-p62, prevents pancreatic cell death. *J Biol Chem* **2011**, *286*, 8308-8324, doi:10.1074/jbc.M110.197301.
18. Ropolo, A.; Grasso, D.; Vaccaro, M.I. Measuring Autophagy in Pancreatitis. *Methods Mol Biol* **2019**, *1880*, 541-554, doi:10.1007/978-1-4939-8873-0_35.
19. Ghanbarpour, A.; Valverde, D.P.; Melia, T.J.; Reinisch, K.M. A model for a partnership of lipid transfer proteins and scramblases in membrane expansion and organelle biogenesis. *Proc Natl Acad Sci U S A* **2021**, *118*, doi:10.1073/pnas.2101562118.
20. Grasso, D.; Sacchetti, M.L.; Bruno, L.; Lo Re, A.; Iovanna, J.L.; Gonzalez, C.D.; Vaccaro, M.I. Autophagy and VMP1 expression are early cellular events in experimental diabetes. *Pancreatology* **2009**, *9*, 81-88, doi:10.1159/000178878.
21. Gilabert, M.; Vaccaro, M.I.; Fernandez-Zapico, M.E.; Calvo, E.L.; Turrini, O.; Secq, V.; Garcia, S.; Moutardier, V.; Lomberk, G.; Dusetti, N.; et al. Novel role of VMP1 as modifier of the pancreatic tumor cell response to chemotherapeutic drugs. *J Cell Physiol* **2013**, *228*, 1834-1843, doi:10.1002/jcp.24343.
22. Ropolo, A.; Catrinacio, C.; Renna, F.J.; Boggio, V.; Orquera, T.; Gonzalez, C.D.; Vaccaro, M.I. A Novel E2F1-EP300-VMP1 Pathway Mediates Gemcitabine-Induced Autophagy in Pancreatic Cancer Cells Carrying Oncogenic KRAS. *Front Endocrinol (Lausanne)* **2020**, *11*, 411, doi:10.3389/fendo.2020.00411.
23. Vanasco, V.; Ropolo, A.; Grasso, D.; Ojeda, D.S.; Garcia, M.N.; Vico, T.A.; Orquera, T.; Quarleri, J.; Alvarez, S.; Vaccaro, M.I. Mitochondrial Dynamics and VMP1-Related Selective Mitophagy in Experimental Acute Pancreatitis. *Front Cell Dev Biol* **2021**, *9*, 640094, doi:10.3389/fcell.2021.640094.
24. Lo Re, A.E.; Fernandez-Barrena, M.G.; Almada, L.L.; Mills, L.D.; Elsawa, S.F.; Lund, G.; Ropolo, A.; Molejon, M.I.; Vaccaro, M.I.; Fernandez-Zapico, M.E. Novel AKT1-GLI3-VMP1 pathway mediates KRAS oncogene-induced autophagy in cancer cells. *J Biol Chem* **2012**, *287*, 25325-25334, doi:10.1074/jbc.M112.370809.
25. Rodriguez, M.E.; Catrinacio, C.; Ropolo, A.; Rivarola, V.A.; Vaccaro, M.I. A novel HIF-1alpha/VMP1-autophagic pathway induces resistance to photodynamic therapy in colon cancer cells. *Photochem Photobiol Sci* **2017**, *16*, 1631-1642, doi:10.1039/c7pp00161d.
26. Karanasios, E.; Walker, S.A.; Okkenhaug, H.; Manifava, M.; Hummel, E.; Zimmermann, H.; Ahmed, Q.; Domart, M.C.; Collinson, L.; Ktistakis, N.T. Autophagy initiation by ULK complex assembly on ER tubulovesicular regions marked by ATG9 vesicles. *Nat Commun* **2016**, *7*, 12420, doi:10.1038/ncomms12420.
27. Panagopoulos, A.; Taraviras, S.; Nishitani, H.; Lygerou, Z. CRL4(Cdt2): Coupling Genome Stability to Ubiquitination. *Trends Cell Biol* **2020**, *30*, 290-302, doi:10.1016/j.tcb.2020.01.005.
28. Leck, Y.C.; Choo, Y.Y.; Tan, C.Y.; Smith, P.G.; Hagen, T. Biochemical and cellular effects of inhibiting Nedd8 conjugation. *Biochem Biophys Res Commun* **2010**, *398*, 588-593, doi:10.1016/j.bbrc.2010.06.128.
29. Levine, B.; Kroemer, G. Biological Functions of Autophagy Genes: A Disease Perspective. *Cell* **2019**, *176*, 11-42, doi:10.1016/j.cell.2018.09.048.
30. Mulcahy Levy, J.M.; Thorburn, A. Autophagy in cancer: moving from understanding mechanism to improving therapy responses in patients. *Cell Death Differ* **2020**, *27*, 843-857, doi:10.1038/s41418-019-0474-7.
31. Sui, X.; Chen, R.; Wang, Z.; Huang, Z.; Kong, N.; Zhang, M.; Han, W.; Lou, F.; Yang, J.; Zhang, Q.; et al. Autophagy and chemotherapy resistance: a promising therapeutic target for cancer treatment. *Cell Death Dis* **2013**, *4*, e838, doi:10.1038/cddis.2013.350.

32. Sun, T.; Liu, Z.; Yang, Q. The role of ubiquitination and deubiquitination in cancer metabolism. *Mol Cancer* **2020**, *19*, 146, doi:10.1186/s12943-020-01262-x.
33. Abbas, T.; Dutta, A. CRL4Cdt2: master coordinator of cell cycle progression and genome stability. *Cell Cycle* **2011**, *10*, 241-249, doi:10.4161/cc.10.2.14530.
34. Itakura, E.; Mizushima, N. p62 Targeting to the autophagosome formation site requires self-oligomerization but not LC3 binding. *J Cell Biol* **2011**, *192*, 17-27, doi:10.1083/jcb.201009067.
35. Leidal, A.M.; Huang, H.H.; Marsh, T.; Solvik, T.; Zhang, D.; Ye, J.; Kai, F.; Goldsmith, J.; Liu, J.Y.; Huang, Y.H.; et al. The LC3-conjugation machinery specifies the loading of RNA-binding proteins into extracellular vesicles. *Nat Cell Biol* **2020**, *22*, 187-199, doi:10.1038/s41556-019-0450-y.
36. Solvik, T.A.; Nguyen, T.A.; Tony Lin, Y.H.; Marsh, T.; Huang, E.J.; Wiita, A.P.; Debnath, J.; Leidal, A.M. Secretory autophagy maintains proteostasis upon lysosome inhibition. *J Cell Biol* **2022**, *221*, doi:10.1083/jcb.202110151.
37. Nazio, F.; Strappazzon, F.; Antonioli, M.; Bielli, P.; Cianfanelli, V.; Bordi, M.; Gretzmeier, C.; Dengjel, J.; Piacentini, M.; Fimia, G.M.; et al. mTOR inhibits autophagy by controlling ULK1 ubiquitylation, self-association and function through AMBRA1 and TRAF6. *Nat Cell Biol* **2013**, *15*, 406-416, doi:10.1038/ncb2708.
38. Xiao, J.; Zhang, T.; Xu, D.; Wang, H.; Cai, Y.; Jin, T.; Liu, M.; Jin, M.; Wu, K.; Yuan, J. FBXL20-mediated Vps34 ubiquitination as a p53 controlled checkpoint in regulating autophagy and receptor degradation. *Genes Dev* **2015**, *29*, 184-196, doi:10.1101/gad.252528.114.
39. Zhang, T.; Dong, K.; Liang, W.; Xu, D.; Xia, H.; Geng, J.; Najafov, A.; Liu, M.; Li, Y.; Han, X.; et al. G-protein-coupled receptors regulate autophagy by ZBTB16-mediated ubiquitination and proteasomal degradation of Atg14L. *Elife* **2015**, *4*, e06734, doi:10.7554/eLife.06734.
40. Shi, C.S.; Kehrl, J.H. TRAF6 and A20 regulate lysine 63-linked ubiquitination of Beclin-1 to control TLR4-induced autophagy. *Sci Signal* **2010**, *3*, ra42, doi:10.1126/scisignal.2000751.
41. Platta, H.W.; Abrahamsen, H.; Thoresen, S.B.; Stenmark, H. Nedd4-dependent lysine-11-linked polyubiquitination of the tumour suppressor Beclin 1. *Biochem J* **2012**, *441*, 399-406, doi:10.1042/BJ20111424.
42. Xu, C.; Feng, K.; Zhao, X.; Huang, S.; Cheng, Y.; Qian, L.; Wang, Y.; Sun, H.; Jin, M.; Chuang, T.H.; et al. Regulation of autophagy by E3 ubiquitin ligase RNF216 through BECN1 ubiquitination. *Autophagy* **2014**, *10*, 2239-2250, doi:10.4161/15548627.2014.981792.
43. Lu, G.; Yi, J.; Gubas, A.; Wang, Y.T.; Wu, Y.; Ren, Y.; Wu, M.; Shi, Y.; Ouyang, C.; Tan, H.W.S.; et al. Suppression of autophagy during mitosis via CUL4-RING ubiquitin ligases-mediated WIPI2 polyubiquitination and proteasomal degradation. *Autophagy* **2019**, *15*, 1917-1934, doi:10.1080/15548627.2019.1596484.
44. Amirfallah, A.; Arason, A.; Einarsson, H.; Gudmundsdottir, E.T.; Freysteinsdottir, E.S.; Olafsdottir, K.A.; Johannsson, O.T.; Agnarsson, B.A.; Barkardottir, R.B.; Reynisdottir, I. High expression of the vacuole membrane protein 1 (VMP1) is a potential marker of poor prognosis in HER2 positive breast cancer. *PLoS One* **2019**, *14*, e0221413, doi:10.1371/journal.pone.0221413.
45. Pan, H.W.; Chou, H.Y.; Liu, S.H.; Peng, S.Y.; Liu, C.L.; Hsu, H.C. Role of L2DTL, cell cycle-regulated nuclear and centrosome protein, in aggressive hepatocellular carcinoma. *Cell Cycle* **2006**, *5*, 2676-2687, doi:10.4161/cc.5.22.3500.
46. Kobayashi, H.; Komatsu, S.; Ichikawa, D.; Kawaguchi, T.; Hirajima, S.; Miyamae, M.; Okajima, W.; Ohashi, T.; Kosuga, T.; Konishi, H.; et al. Overexpression of denticleless E3 ubiquitin protein ligase homolog (DTL) is related to poor outcome in gastric carcinoma. *Oncotarget* **2015**, *6*, 36615-36624, doi:10.18632/oncotarget.5620.
47. Benamar, M.; Guessous, F.; Du, K.; Corbett, P.; Obeid, J.; Gioeli, D.; Slingluff, C.L., Jr.; Abbas, T. Inactivation of the CRL4-CDT2-SET8/p21 ubiquitylation and degradation axis underlies the therapeutic efficacy of pevonedistat in melanoma. *EBioMedicine* **2016**, *10*, 85-100, doi:10.1016/j.ebiom.2016.06.023.
48. Wei, D.; Li, H.; Yu, J.; Sebolt, J.T.; Zhao, L.; Lawrence, T.S.; Smith, P.G.; Morgan, M.A.; Sun, Y. Radiosensitization of human pancreatic cancer cells by MLN4924, an investigational NEDD8-activating enzyme inhibitor. *Cancer Res* **2012**, *72*, 282-293, doi:10.1158/0008-5472.CAN-11-2866.

49. Rossi, M.; Duan, S.; Jeong, Y.T.; Horn, M.; Saraf, A.; Florens, L.; Washburn, M.P.; Antebi, A.; Pagano, M. Regulation of the CRL4(Cdt2) ubiquitin ligase and cell-cycle exit by the SCF(Fbxo11) ubiquitin ligase. *Mol Cell* **2013**, *49*, 1159-1166, doi:10.1016/j.molcel.2013.02.004.